

A New Gravitational Wave Verification Source^{*}

Mukremin Kilic¹, Warren R. Brown², A. Gianninas¹, J. J. Hermes³,
Carlos Allende Prieto^{4,5}, and S. J. Kenyon²

¹*Department of Physics and Astronomy, University of Oklahoma, 440 W. Brooks St., Norman, OK, 73019, USA*

²*Smithsonian Astrophysical Observatory, 60 Garden St, Cambridge, MA 02138, USA*

³*Department of Physics, University of Warwick, Coventry CV4 7AL, UK*

⁴*Instituto de Astrofísica de Canarias, E-38205 La Laguna, Tenerife, Spain*

⁵*Departamento de Astrofísica, Universidad de La Laguna, E-38206 La Laguna, Tenerife, Spain*

16 June 2014

ABSTRACT

We report the discovery of a detached 20 min orbital period binary white dwarf. WD 0931+444 (SDSS J093506.93+441106.9) was previously classified as a WD + M dwarf system based on its optical spectrum. Our time-resolved optical spectroscopy observations obtained at the 8m Gemini and 6.5m MMT reveal peak-to-peak radial velocity variations of $\approx 400 \text{ km s}^{-1}$ every 20 min for the WD, but no velocity variations for the M dwarf. In addition, high-speed photometry from the McDonald 2.1m telescope shows no evidence of variability nor evidence of a reflection effect. An M dwarf companion is physically too large to fit into a 20 min orbit. Thus, the orbital motion of the WD is almost certainly due to an invisible WD companion. The M dwarf must be either an unrelated background object or the tertiary component of a hierarchical triple system. WD 0931+444 contains a pair of WDs, a $0.32 M_{\odot}$ primary and a $\geq 0.14 M_{\odot}$ secondary, at a separation of $\geq 0.19 R_{\odot}$. After J0651+2844, WD 0931+444 becomes the second-shortest period detached binary WD currently known. The two WDs will lose angular momentum through gravitational wave radiation and merge in $\leq 9 \text{ Myr}$. The $\log h \simeq -22$ gravitational wave strain from WD 0931+444 is strong enough to make it a verification source for gravitational wave missions in the milli-Hertz frequency range, e.g. the evolved Laser Interferometer Space Antenna (*eLISA*), bringing the total number of known *eLISA* verification sources to nine.

Key words: binaries: close — white dwarfs — stars: individual (SDSS J093506.93+441106.9, WD 0931+444) — gravitational waves

1 INTRODUCTION

Short period binary WDs are expected to dominate the gravitational wave foreground at mHz frequencies. Nelemans (2013) predicts $\sim 10^8$ double WDs in the Galaxy, including several thousand sources that should be individually detected by *eLISA* (Amaro-Seoane et al. 2012). However,

there are only eight *eLISA* verification sources currently known. All but one of these are AM Canum Venaticorum binaries (e.g., Solheim 2010) with orbital periods ranging from 5 to 27 min. The remaining system is the 12-min orbital period detached binary J0651+2844 (Brown et al. 2011; Hermes et al. 2012).

Low-mass ($M < 0.45 M_{\odot}$) WDs are signposts of short period binary systems (e.g., Marsh et al. 1995; Napiwotzki et al. 2007). We established a radial velocity program, the Extremely-Low Mass (ELM) Survey (Brown et al. 2010, 2012, 2013; Kilic et al. 2010, 2011, 2012), to identify short period binary WDs that are strong gravitational wave sources and potential progenitors of Type Ia and Ia supernovae (Bildsten et al. 2007; Shen & Bildsten 2009; Kilic et al. 2014). The ELM Survey has so far discovered 55 binaries, all with $P \lesssim 1 \text{ d}$, including 32 that will merge within a Hubble time (Gianninas et al. 2014). Three

^{*} Based on observations obtained at the Gemini and MMT observatories. Gemini is operated by the Association of Universities for Research in Astronomy, Inc., under a cooperative agreement with the NSF on behalf of the Gemini partnership: the National Science Foundation (United States), the National Research Council (Canada), CONICYT (Chile), the Australian Research Council (Australia), Ministério da Ciência, Tecnologia e Inovação (Brazil) and Ministerio de Ciencia, Tecnología e Innovación Productiva (Argentina). The MMT is a joint facility of the Smithsonian Institution and the University of Arizona.

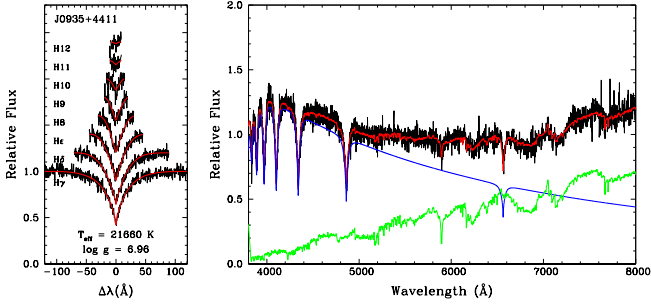


Figure 1. Left Panel: Model fits (red lines) to the Balmer line profiles of WD 0931+444 from the MMT spectroscopy. Right Panel: Model fits to the SDSS spectroscopy, including the contribution from the WD (blue line) and M dwarf (green line).

of these have orbital periods less than an hour; J0651+2844, J0106–1000, and J1630+4233.

We have recently extended our search for ELM WDs to the Sloan Digital Sky Survey Data Release 10 (SDSS DR10, Ahn et al. 2014). We fit all available DR10 spectroscopy for stellar sources with WD model spectra (Koester 2010) to identify ELM WDs with $5 \leq \log g \leq 7$ and $M \leq 0.3 M_{\odot}$. Here we present optical spectroscopy and photometry of one of these sources, the relatively bright ($g = 17.7$ mag) SDSS J093506.93+441106.9 (WD 0931+444).

Usher et al. (1982) identified WD 0931+444 as a UV-excess object in the Palomar Schmidt plates, and Mitchell & Usher (2004) confirmed it as a DA WD based on optical spectroscopy. However, the SDSS observations clearly show a composite spectrum of a DA WD plus an M dwarf (Kleinman et al. 2013). Silvestri et al. (2006), Rebassa-Mansergas et al. (2007, 2010), and Heller et al. (2009) classify WD 0931+444 as a low-mass WD with $T_{\text{eff}} \sim 20,000\text{K}$, $\log g \approx 7$, and an M1 dwarf companion. Rebassa-Mansergas et al. (2007) find an average mass and radius of $M = 0.46 M_{\odot}$ and $R = 0.43 \pm 0.09 R_{\odot}$ for M1 dwarfs, which implies a distance of 1440 ± 340 pc for the M dwarf in WD 0931+444. Rebassa-Mansergas et al. (2010) revise the distance to $\approx 1150 \pm 220$ pc, which is 2.2σ farther away than the WD (see §3.1). However, there seems to be a systematic effect that leads to overestimating the M dwarf distances in DA + M systems (see Rebassa-Mansergas et al. 2010). For example, the distance estimates for the WDs and M dwarfs in the 58 Post-Common-Envelope-Binaries presented in Nebot Gómez-Morán et al. (2011) differ by as much as 3σ . Hence, the inconsistent distance estimates for the WD and M dwarf do not rule out physical association. Rebassa-Mansergas et al. (2007) also point out that the M dwarf in WD 0931+444 has a poorly defined Na I doublet, possibly due to orbital motion. If so, the relatively hot WD would cause significant heating of the secondary star, which would be detected as a reflection effect in the optical lightcurve.

Our radial velocity and high-speed photometry demonstrate that WD 0931+444 contains a pair of WDs with an orbital period of only 20 min, and that the M dwarf is not a member of this binary. In Section 2 we describe our spectroscopic and photometric observations. In Sections 3 and 4 we constrain the physical parameters of this system and discuss the nature and future evolution of WD 0931+444. We conclude in Section 5.

Table 1. Radial velocity measurements for WD 0931+444. The full table is available online.

HJD–2456500 (days)	v_{helio} (km s $^{-1}$)
97.029593	104.34 ± 23.31
98.029345	191.50 ± 30.83
99.023102	199.16 ± 25.51
99.023970	84.95 ± 35.74
99.024850	-16.74 ± 39.36

2 OBSERVATIONS

We used the 6.5m MMT with the Blue Channel spectrograph to obtain medium resolution spectroscopy of WD 0931+444 in 2013 November and 2014 March. The former observations used the 832 line mm $^{-1}$ grating in second order, providing wavelength coverage from 3600 Å to 4500 Å and a spectral resolution of 1.2 Å. The latter observations used the 1200 line mm $^{-1}$, providing wavelength coverage from 5640 Å to 6940 Å and a spectral resolution of 1.5 Å. We obtained all observations at the parallactic angle.

We obtained follow-up optical spectroscopy using the 8m Gemini-North telescope with the Gemini Multi-Object Spectrograph (GMOS) in 2014 March as part of program GN-2013B-DD-9. We obtained a sequence of 32×150s exposures with the R831 grating and a 0.5'' slit, providing wavelength coverage from 5460 Å to 7560 Å and a resolving power of 3720. We also obtained a sequence of 20×120 s exposures with the B1200 grating and a 0.5'' slit, providing wavelength coverage from 3700 Å to 5150 Å and a resolving power of 3635. Each spectrum has a comparison lamp exposure taken within 10 min of the observation time. We flux-calibrate using blue spectrophotometric standards (Massey et al. 1988), and measure radial velocities using the cross-correlation package RVSAO.

We acquired high speed photometry of WD 0931+444 using the McDonald 2.1m Telescope with the Puoko-nui North camera (Chote et al. 2014) over five nights in 2013 December. We obtained images through both a BG40 filter (8.2 h) and an SDSS z -band filter (5.8 h) to look for variations in the light curve for the WD and M dwarf, respectively.

3 RESULTS

3.1 The ELM WD

Figure 1 shows the optical spectrum of WD 0931+444 along with our model fits. The optical spectrum is dominated by the WD below 5000 Å, which enables us to use the Balmer lines to constrain the physical parameters of the WD precisely. We use the H γ -H12 lines in our MMT spectra and an extended model atmosphere grid based on the Bergeron et al. (1995) models, with recent improvements presented in Tremblay & Bergeron (2009), to constrain the atmospheric parameters of the WD. The best-fit model has $T_{\text{eff}} = 21660 \pm 380$ K and $\log g = 6.96 \pm 0.05$. The recent evolutionary calculations by Althaus et al. (2013) indicate that WD 0931+444 is an $M = 0.32 \pm 0.02 M_{\odot}$ and $R = 0.031 \pm 0.003 R_{\odot}$ WD at a distance of 660 ± 70 pc.

The right panel in Figure 1 shows composite WD + M

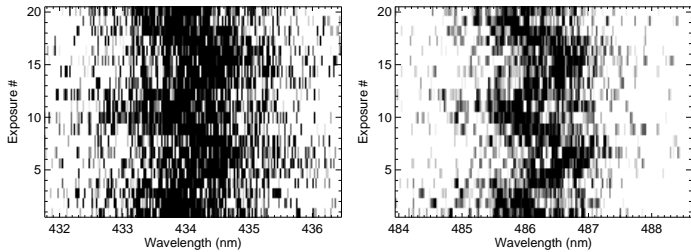


Figure 2. Gemini time-resolved spectroscopy of $H\gamma$ (left panel) and $H\beta$ lines (right panel) over 45 min. Both lines clearly show a 20 min periodicity.

dwarf model fits to the SDSS spectrum of WD 0931+444. We use the best-fit WD model to subtract out the contribution from the WD and use the Bochanski et al. (2007) templates to fit the contribution from the M dwarf. The best-fit template is M1.5, consistent with the previous analyses by Silvestri et al. (2006), Heller et al. (2009), and Rebassa-Mansergas et al. (2010). This spectral type is also consistent with the infrared data from the Two Micron All Sky Survey (Cutri et al. 2003) and the Wide-Field Infrared Survey Explorer (Wright et al. 2010).

3.2 The Orbital Period

Figure 2 shows Gemini time-resolved spectroscopy of $H\gamma$ and $H\beta$ lines over 45 min. $H\beta$ and higher order Balmer lines are relatively clean, with no evidence of significant contamination or activity from the M dwarf. All of the Balmer lines clearly show evidence of a 20 min orbital period.

Figure 3 shows 55 radial velocity measurements for WD 0931+444 obtained from $H\gamma$ through $H12$ lines. Table 1 lists these velocities. We compute the best-fit orbital elements using the code of Kenyon & Garcia (1986), and perform a Monte Carlo analysis to verify the uncertainties in the orbital parameters (see Brown et al. 2012, for details). WD 0931+444 exhibits radial velocity variations with a semi-amplitude of $K = 185.4 \pm 3.2 \text{ km s}^{-1}$ and orbital period of $P = 0.01375 \pm 0.00051 \text{ d}$, or $19.8 \pm 0.7 \text{ min}$, with a significant alias at 20.4 min. The observed velocity amplitude is underestimated, however, because our 2 min long exposures span 10% of the orbital phase. The corrected velocity semi-amplitude is $K = 198.5 \pm 3.2 \text{ km s}^{-1}$. After correcting for the gravitational redshift of the WD (6.6 km s^{-1}), the systemic velocity is $74.3 \pm 2.3 \text{ km s}^{-1}$. The mass function is $f = 0.0111 \pm 0.0007 M_{\odot}$, which implies an $M \geq 0.13 M_{\odot}$ companion at a separation of $0.19 R_{\odot}$.

At an inclination angle of $i = 90^{\circ}$, a $0.13 M_{\odot}$ companion would have a Roche-lobe radius of $0.056 R_{\odot}$ (Eggleton 1983). This is smaller than the radii for all known M dwarfs (see Table 5 in Rebassa-Mansergas et al. 2007). Hence, if the orbital motion of WD 0931+444 is due to an M dwarf, such a companion would fill its Roche lobe, yet there is no evidence of mass transfer in this system. In fact, no main-sequence star can fit into this orbit; the orbital period of this system is significantly shorter than the period minimum for cataclysmic variables ($\approx 78 \text{ min}$, Hellier 2001). Clearly, the visible M dwarf in WD 0931+444 cannot be a binary companion of the WD. Based on the mass function alone, the probability of a $M \leq 1.4 M_{\odot}$ companion is 97.5%. Hence, the companion is almost certainly another WD.

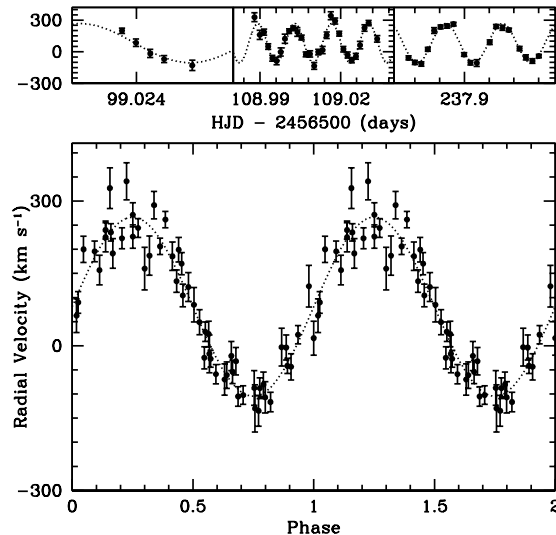


Figure 3. The radial velocities of the Balmer lines in WD 0931+444. The bottom panel shows all of these data points phased with the best-fit period. The dotted line represents the best-fit model for a circular orbit with a period of 0.01375 d.

3.3 The M dwarf in WD 0931+444

Figure 4 shows the Gemini time-resolved spectroscopy of the Na I doublet and the $H\alpha$ line. There is no evidence of any metal-pollution in the DA WD, hence the Na I doublet is clearly from the M dwarf. If the M dwarf was associated with the 20 min binary, given the mass ratio of the two stars, we would expect to see peak-to-peak velocity variations of 276 km s^{-1} . On the contrary, the velocity of the Na I doublet is consistent with $\Delta v = 0 \pm 4 \text{ km s}^{-1}$ in all of the Gemini and MMT spectra. Forcing a 20-min periodicity, the best-fit velocity semi-amplitude is 3.3 km s^{-1} . Clearly, the M dwarf does not display any significant radial velocity variability.

The right panel of Figure 4 is perhaps more revealing. This figure displays two components for the $H\alpha$ line. The first one, from the M dwarf, is stationary. While the second one, from the WD, shows significant velocity variations. The $H\alpha$ line from the WD clearly goes through 4+ orbital cycles in this figure, consistent with the orbital period of 20 min, as measured from the rest of the Balmer lines (see Fig. 2).

3.4 The Light Curve

Figure 5 shows the McDonald 2.1m telescope light curve of WD 0931+444. The fourier transforms of the blue-sensitive BG40 and the red-sensitive SDSS z -band data are also shown. These light curves do not reveal any significant photometric variability. There is a marginal peak ($< 3\sigma$) at 1203.6 s in the BG40 filter data. This is consistent with variations at the orbital period, which may be due to the relativistic beaming effect. Similarly there is a marginal peak in the z -band data at 1758.2 s. No variations are expected at that frequency, hence this marginal signal is most likely due to noise from atmospheric variability in the z -band.

Assuming that the secondary star has a radius comparable to the ELM WD, the lack of eclipses in our photometry require $i \leq 70^{\circ}$, which implies a $M \geq 0.14 M_{\odot}$ WD companion. For $i \leq 70^{\circ}$ and the limb- and gravity-darkening coefficients of $u = 0.34$ (Gianninas et al. 2013) and $\tau = 0.48$,

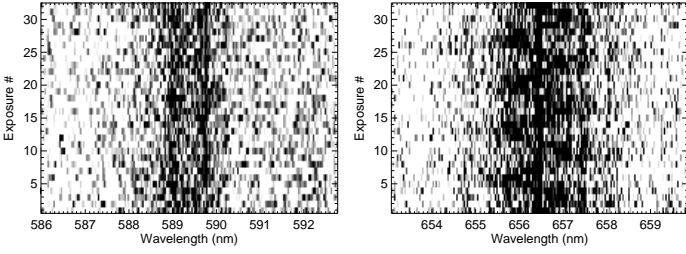


Figure 4. Gemini time-resolved spectroscopy of the Na I doublet (left panel) and the H α line (right panel) over 90 min. The Na I lines and the H α line from the M dwarf are stationary, whereas the H α line from the WD clearly shows a 20 min periodicity.

respectively, we expect $\leq 0.25\%$ ellipsoidal variations in the BG40 filter due to tidal distortions of the primary. This amplitude is below our detection threshold, so the lack of a signal at half the orbital period does not provide any new constraints on the inclination of the binary.

The absence of a reflection effect is additional evidence that the M dwarf does not orbit the WD. For comparison, HS 2043+0615 is a $T_{\text{eff}} \approx 26,000$ K subdwarf star with a $0.18\text{--}0.34 M_{\odot}$ M dwarf companion in a 0.3 d binary. This system shows 0.15 mag brightness variations due to the reflection effect (Geier et al. 2014). Similarly, SDSS J162256.66+473051.1 contains a subdwarf star with a heated brown dwarf companion in a 0.07 d orbit, and shows a $\sim 10\%$ reflection effect (Schaffenroth et al. 2014). Yet, there is no evidence of a reflection effect for WD 0931+444 in our photometry. This further reinforces our determination that the M dwarf is not in the 20-min orbit with the visible WD.

4 DISCUSSION

4.1 A New Verification Binary

Our optical spectroscopy and photometry demonstrate that WD 0931+444 is a 20 min orbital period detached double WD. Along with J0106–1000, J0651+2844, and J1630+4233, WD 0931+444 becomes the fourth detached WD binary known to have a period less than an hour. The two WDs in this system will merge in ≤ 9 Myr. After J0651, WD 0931+444 becomes the second quickest WD merger system currently known.

At a distance of 660 pc and $i \leq 70^\circ$, we expect the gravitational wave strain at Earth $\log h \geq -22.17$ at $\log \nu$ (Hz) = -2.77 (Roelofs et al. 2007). Hence, WD 0931+444 is clearly a verification source for *eLISA*, bringing the total number of known *eLISA* verification sources to nine.

When the mass transfer starts, WD 0931+444 will most likely have unstable mass transfer (Marsh et al. 2004). However, the merger outcome is uncertain because of the unknown inclination angle and the companion mass. For a relatively high inclination angle of $i \approx 70^\circ$, the companion would be a very low-mass WD with $M = 0.14 M_{\odot}$, and the merger will lead to a single He-burning subdwarf star. For an inclination of $i = 31^\circ$, WD 0931+444 would be an equal mass binary with a merger time of 4.4 Myr, and $\log h = -21.6$. This is similar to the gravitational wave strain from the verification binary HP Lib (Nelemans 2006). The non-detection of the secondary WD in our spectroscopy implies that the companion is cooler (like CS 41177, Bours et al. 2014) and/or more massive (like J0651, Brown et al. 2011). Therefore, the

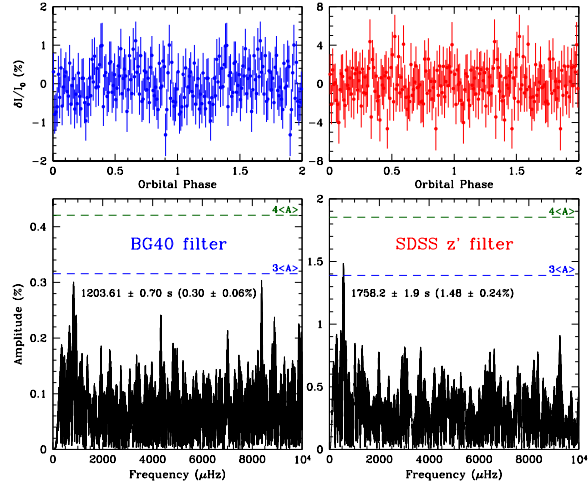


Figure 5. High speed photometry of WD 0931+444 in the BG40 (left panel) and the z -band filter (right panel). The light curve is binned into 100 phase bins and folded at the best-fit orbital period from the radial velocity measurements. The bottom panels show the Fourier transform of both datasets.

gravitational wave strain of WD 0931+444 may be even higher than this estimate, potentially making it one of the best verification sources known.

4.2 Is WD 0931+444 a Triple System?

There is growing interest in triples containing an inner double WD binary. Perets & Kratter (2012) suggest that mass loss in an evolving triple system leads to orbital instability, triggering close encounters or collisions in the system. This mechanism could explain prompt supernovae Ia, and contribute to the Ia event rate (Kushnir et al. 2013). However, Hamers et al. (2013) find this rate to be low.

To explore the eccentricity of the WD 0931+444 binary, we fit both circular and eccentric orbits to the radial velocity data. The 3σ upper limit on eccentricity is $e = 0.02$, and the Lucy & Sweeney (1971) test strongly prefers a circular orbit. This suggests that the Kozai mechanism is not important for WD 0931+444, and we are yet to find a triple system containing an eccentric double WD inner binary.

Given the size of the orbit ($0.19 R_{\odot}$), and the lack of evidence for mass transfer and a reflection effect, the M dwarf that contaminates the SDSS spectrum of WD 0931+444 cannot be a member of the 20 min period binary. The distance estimate also puts the M dwarf significantly further away than the WD, though the distance uncertainty is rather large. Cross-correlating with a template spectrum of an inactive M1 dwarf (Bochanski et al. 2007), we measure velocities of -47 ± 9 and -37 ± 13 km s $^{-1}$ for the Na I doublet from the Gemini and MMT spectra, respectively. These are significantly different than the systemic velocity of the WD binary (74.3 ± 2.3 km s $^{-1}$). Hence, the M dwarf is likely a background source.

Based on six epochs from the USNO-B and the SDSS, Munn et al. (2004) measure a proper motion of $(\mu_{\alpha} \cos \delta, \mu_{\delta}) = (-19.9, -0.8)$ mas yr $^{-1}$. WD 0931+444 is unresolved in the Palomar plates and the SDSS images. If the proper motion measurement is correct, WD 0931+444 would have moved only $1''$ between the first Palomar observations and the SDSS. Hence, the current proper motion

measurements are inconclusive in deciding if the M dwarf is the tertiary component of the WD 0931+444 system. If the M dwarf is a background object, the Hubble Space Telescope observations may be able to resolve the WD and the M dwarf and confirm or rule out any physical association based on common proper motion.

5 CONCLUSIONS

We identify WD 0931+444 as a new *eLISA* verification source, only the ninth such system known. WD 0931+444 is a 20 min orbital period detached binary WD, the second-quickest merger system currently known. It contains a $0.32 M_{\odot}$ WD and a $\geq 0.14 M_{\odot}$ companion. The M dwarf in this system may or may not be associated with WD 0931+444, and we propose follow-up proper motion measurements to distinguish between the two scenarios. Since the companion WD is not detected in our spectroscopy or photometry, it is likely cooler and/or more massive than the ELM WD. A more massive companion would make it one of the strongest sources of gravitational radiation currently known.

ACKNOWLEDGEMENTS

We gratefully acknowledge the support of the NSF under grant AST-1312678. JJH acknowledges funding from the European Research Council under the European Union's Seventh Framework Programme (FP/2007-2013) / ERC Grant Agreement n. 320964 (WDTracer). We thank the Gemini staff, including Atsuko Nitta and Nancy Levenson, for help with our observing program.

REFERENCES

- Ahn, C. P., Alexandroff, R., Allende Prieto, C., et al. 2014, *ApJS*, 211, 17
- Althaus, L. G., Miller Bertolami, M. M., & Córscico, A. H. 2013, *A&A*, 557, A19
- Amaro-Seoane, P., Aoudia, S., Babak, S., et al. 2012, *Classical and Quantum Gravity*, 29, 124016
- Bergeron, P., Wesemael, F., & Beauchamp, A. 1995, *PASP*, 107, 1047
- Bildsten, L., Shen, K. J., Weinberg, N. N., & Nelemans, G. 2007, *ApJ*, 662, L95
- Bochanski, J. J., West, A. A., Hawley, S. L., & Covey, K. R. 2007, *AJ*, 133, 531
- Bours, M. C. P., Marsh, T. R., Parsons, S. G., et al. 2014, *MNRAS*, 438, 3399
- Brown, W. R., Kilic, M., Allende Prieto, C., & Kenyon, S. J. 2010, *ApJ*, 723, 1072
- Brown, W. R., Kilic, M., Hermes, J. J., et al. 2011, *ApJ*, 737, L23
- Brown, W. R., Kilic, M., Allende Prieto, C., & Kenyon, S. J. 2012, *ApJ*, 744, 142
- Brown, W. R., Kilic, M., Allende Prieto, C., Gianninas, A., & Kenyon, S. J. 2013, *ApJ*, 769, 66
- Chote, P., Sullivan, D. J., Brown, R., et al. 2014, *MNRAS*, 440, 1490
- Cutri, R. M., Skrutskie, M. F., van Dyk, S., et al. 2003, *VizieR Online Data Catalog*, 2246, 0
- Eggleton, P. P. 1983, *ApJ*, 268, 368
- Geier, S., Østensen, R. H., Heber, U., et al. 2014, *A&A*, 562, A95
- Gianninas, A., Strickland, B. D., Kilic, M., & Bergeron, P. 2013, *ApJ*, 766, 3
- Gianninas, A., Hermes, J. J., Brown, W. R., et al. 2014, *ApJ*, 781, 104
- Hamers, A. S., Pols, O. R., Claeys, J. S. W., & Nelemans, G. 2013, *MNRAS*, 430, 2262
- Heller, R., Homeier, D., Dreizler, S., & Østensen, R. 2009, *A&A*, 496, 191
- Hellier, C. 2001, *Cataclysmic Variable Stars*, Springer, 2001
- Hermes, J. J., Kilic, M., Brown, W. R., et al. 2012, *ApJ*, 757, L21
- Kenyon, S. J. & Garcia, M. R. 1986, *AJ*, 91, 125
- Kilic, M., Brown, W. R., Allende Prieto, C., Kenyon, S. J., & Panei, J. A. 2010, *ApJ*, 716, 122
- Kilic, M., Brown, W. R., Allende Prieto, C., et al. 2011, *ApJ*, 727, 3
- Kilic, M., Brown, W. R., Allende Prieto, C., et al. 2012, *ApJ*, 751, 141
- Kilic, M., Hermes, J. J., Gianninas, A., et al. 2014, *MNRAS*, 438, L26
- Kleinman, S. J., Kepler, S. O., Koester, D., et al. 2013, *ApJS*, 204, 5
- Koester, D. 2010, *Memorie della Societa Astronomica Italiana*, 81, 921
- Kushnir, D., Katz, B., Dong, S., Livne, E., & Fernández, R. 2013, *ApJ*, 778, L37
- Lucy, L. B., & Sweeney, M. A. 1971, *AJ*, 76, 544
- Munn, J. A., Monet, D. G., Levine, S. E., et al. 2004, *AJ*, 127, 3034
- Marsh, T. R., Dhillon, V. S., & Duck, S. R. 1995, *MNRAS*, 275, 828
- Marsh, T. R., Nelemans, G., & Steeghs, D. 2004, *MNRAS*, 350, 113
- Massey, P., Strobel, K., Barnes, J. V., & Anderson, E. 1988, *ApJ*, 328, 315
- Mitchell, K. J., & Usher, P. D. 2004, *ApJS*, 153, 119
- Napiwotzki, R., Karl, C. A., Nelemans, G., et al. 2007, 15th European Workshop on White Dwarfs, 372, 387
- Nebot Gómez-Morán, A., Gänsicke, B. T., Schreiber, M. R., et al. 2011, *A&A*, 536, A43
- Nelemans, G. 2006, 6th International LISA Symposium, 873, 397
- Nelemans, G. 2013, 9th LISA Symposium, 467, 27
- Perets, H. B., & Kratter, K. M. 2012, *ApJ*, 760, 99
- Rebassa-Mansergas, A., Gänsicke, B. T., Rodríguez-Gil, P., Schreiber, M. R., & Koester, D. 2007, *MNRAS*, 382, 1377
- Rebassa-Mansergas, A., Gänsicke, B. T., Schreiber, M. R., Koester, D., & Rodríguez-Gil, P. 2010, *MNRAS*, 402, 620
- Roelofs, G. H. A., Groot, P. J., Benedict, G. F. et al. 2007, *ApJ*, 666, 1174
- Schaffneroth, V., Geier, S., Heber, U., et al. 2014, *A&A*, 564, A98
- Shen, K. J., & Bildsten, L. 2009, *ApJ*, 699, 1365
- Silvestri, N. M., Hawley, S. L., West, A. A., et al. 2006, *AJ*, 131, 1674
- Solheim, J.-E. 2010, *PASP*, 122, 1133
- Tremblay, P.-E., & Bergeron, P. 2009, *ApJ*, 696, 1755
- Usher, P. D., Mattson, D., & Warnock, A., III 1982, *ApJS*, 48, 51
- Wright, E. L., Eisenhardt, P. R. M., Mainzer, A. K., et al. 2010, *AJ*, 140, 1868